Molecular Mechanisms of Lymphocyte Homing to Peripheral Lymph Nodes

By R. Aaron Warnock,* Sanaz Askari,‡ Eugene C. Butcher,* and Ulrich H. von Andrian‡

*From the *Laboratory of Immunology and Vascular Biology, Department of Pathology, Stanford University, Stanford, California 94305, and the Veterans Affairs Palo Alto Health Care Systems, Palo Alto, California 94304; and ‡The Center for Blood Research and the Department of Pathology, Harvard Medical School, Boston, Massachusetts 02115*

Summary

To characterize the adhesion cascade that directs lymphocyte homing to peripheral lymph nodes (PLNs), we investigated the molecular mechanisms of lymphocyte interactions with the microvasculature of subiliac lymph nodes. We found that endogenous white blood cells and adoptively transferred lymph node lymphocytes (LNCs) tethered and rolled in postcapillary high endothelial venules (HEVs) and to a lesser extent in collecting venules. Similarly, firm arrest occurred nearly exclusively in the paracortical HEVs. Endogenous polymorphonuclear (PMNs) and mononuclear leukocytes (MNLs) attached and rolled in HEVs at similar frequencies, but only MNLs arrested suggesting that the events downstream of primary rolling interactions critically determine the specificity of lymphocyte recruitment. Antibody inhibition studies revealed that L-selectin was responsible for attachment and rolling of LNCs, and that LFA-1 was essential for sticking. LFA-1–dependent arrest was also abolished by pertussis toxin, implicating a requirement for $G\alpha_{i-}$-protein–linked signaling. α4 integrins, which play a critical role in lymphocyte homing to Peyer's Patches, made no significant contribution to attachment, rolling, or sticking in resting PLNs. Velocity analysis of interacting LNCs revealed no detectable contribution by LFA-1 to rolling. Taken together, our results suggest that lymphocyte–HEV interactions within PLNs are almost exclusively initiated by L-selectin followed by a G protein–coupled lymphocyte-specific activation event and activation-induced engagement of LFA-1. These events constitute a unique adhesion cascade that dictates the specificity of lymphocyte homing to PLNs.

The surveillance of the body for foreign antigens is a critical function of the immune system. Lymphocytes migrate from the blood into tissues and secondary lymphoid organs, and return back to the blood via lymph vessels and the thoracic duct (1). The majority of lymphocytes are capable of tissue selective trafficking (termed "homing"), recognizing organ-specific adhesion molecules on specialized endothelial cells (2). Tissue-specific homing is thought to control the extent and scope of immune responses, and to account for the regional compartmentalization of immune system functions (3).

A multistep model for leukocyte homing has been proposed (4–6), and aspects of it have been confirmed by various in vitro and in vivo models (7–11). Leukocytes are specifically recruited by combinatorial molecular events: blood-borne cells use primary adhesion molecules to tether and roll on the luminal wall of postcapillary venules, and to encounter and rapidly transduce signals to upregulate secondary adhesion molecules, which then mediate firm arrest. Thus, a variety of adhesive and/or signaling events are used in unique combinations to achieve tissue and subset specificity of homing.

In situ microscopy experiments have demonstrated that such a multistep model applies to lymphocyte homing to Peyer's patches (PPs)[1]. Bargatze et al. found that initial attachment in PPs is L-selectin–dependent, and that established rolling involves both L-selectin and α4β7 integrins that interact with the mucosal addressin, MAdCAM-1 (11). Recent studies in gene-targeted mice have confirmed these distinct but overlapping functions for L-selectin and α4β7

[1]*Abbreviations used in this paper:* BCECF, 2′7′,-bis-(2-carboxyethyl)-5(and 6) carboxyfluorescein; cRPMI, RPMI 1640 + 10% bovine calf serum; HEV, high endothelial venule; LNC, lymph node lymphocyte; MLN, mesenteric lymph node; MNL, mononuclear lymphocyte; MTX, mutant pertussis toxin; PP, Peyer's patch; PLN, peripheral lymph nodes; PNAd, peripheral node addressin; PTX, pertussis toxin; V_{blood}, mean blood flow velocity; V_{fast}, mean fast cell velocity; V_{rel}, relative rolling velocity; V_{roll}, rolling velocity; WBC, white blood cell.

(12, 13). Subsequent arrest of rolling cells is mediated by $\alpha 4\beta 7$ and LFA-1 integrins, and requires a G protein–linked signal that is inhibited by lymphocyte treatment with pertussis toxin (PTX; reference 9). Thus, in PPs, lymphocyte homing requires a cascade of four distinct molecular steps.

A similar multistep adhesion cascade may govern lymphocyte homing to peripheral lymph nodes (PLNs). For example, L-selectin deficiency in mice or treatment of wild-type animals with mAbs to L-selectin or peripheral node addressin (PNAd), the high endothelial venule (HEV)–specific ligand for L-selectin, resulted in impaired lymphocyte homing to PLNs (12, 14–18). Anti–LFA-1 mAbs also reduced homing to PLNs, and PLNs in LFA-1–deficient mice were reportedly smaller than those in heterozygous littermates (19, 20). Finally, treatment of lymphocytes with PTX inhibited migration to PLNs (21), and phenotypically mature thymocytes expressing transgenic PTX homed poorly in adoptive transfer experiments (22). Thus, lymphocyte homing to PLNs appears to require at least three molecular events: L-selectin binding to PNAd; G protein–mediated signaling; and engagement of LFA-1. The spatial and temporal coordination of these events during lymphocyte–HEV interactions has not been examined in vivo.

We have used a novel technique to visualize and dissect interactions of lymphocytes with HEVs in subiliac PLNs of mice. Our findings confirm that lymphocyte homing to PLN-HEVs involves a coordinated multistep process, define important differences from previously described adhesion cascades that mediate homing to other tissues, and help explain the unique recruitment of lymphocyte subsets to PLNs.

Materials and Methods

Reagents. FITC-dextran (10 mg/ml; 150 kD mol mass; Sigma Chemical Co., St. Louis, MO) and rhodamine 6G (2 mg/ml; Molecular Probes, Inc., Eugene, OR) were diluted in saline and undissolved particles were removed by centrifugation; both reagents were freshly prepared for each experiment. 2′7′,-bis-(2-carboxyethyl)-5(and 6) carboxyfluorescein (BCECF; Molecular Probes, Inc.) was prepared as a 0.5 mg/ml stock solution in DMSO and used within 1 wk. EDTA, PMA, and PTX were all from Sigma Chemical Co. Mutant PTX (MTX) with a two amino acid substitution (PT9K129G; reference 23) was a gift of Dr. Rino Rappuoli (IRIS, Chiron Vaccines Immunobiological Research Institute, Sienna, Italy).

Monoclonal Antibodies. mAbs Mel-14 (rat IgG2a, anti–murine L-selectin; reference 14) and MECA 79 (rat IgM, anti-PNAd; reference 15) were generated in our laboratories. Hybridoma cells for these mAbs as well as mAbs Tib 213 (rat IgG2b, anti–murine CD11a; reference 24) and PS/2 (rat IgG2b, anti–murine $\alpha 4$, from American Type Culture Collection, Rockville, MD) were purified from culture supernatant. mAbs were stored at −70°C in endotoxin-free saline at 1 mg/ml. For inhibition studies, 50 μg of antibody was used to preincubate lymphocytes (5–10 × 10^6 cells) in 0.3–0.5 ml RPMI 1640 (Biowhittaker, Walkersville, MD), + 10% bovine calf serum (cRPMI) for 10 min. Animals were given an additional 50 μg intravenously 5 min before cell injection to ensure saturating circulating mAb levels. FITC-conjugated mAbs to murine CD3 and B220 were from PharMingen (San Diego, CA).

Lymphocyte Isolation and Treatment. Lymph node cells (LNCs) were freshly isolated from PLNs (axillary, brachial, cervical, and subiliac) and mesenteric (M) LNs. Cells were washed and resuspended to 1–2 × 10^7 cells/ml in warm cRPMI. Representative samples were stained with FITC-conjugated mAbs to T and B cell markers (CD3 and B220, respectively) and determined by flow cytometry to be ~95% lymphocytes.

For fluorescent labeling, 10 ml of LNCs was incubated with 5 μl BCECF for 20 min at 37°C. Lymphocytes were centrifuged through 5 ml of warm bovine calf serum and supernatant was discarded. The pellet was resuspended to 1–2 × 10^7 cells/ml in warm cRPMI. Aliquots of LNCs were pretreated with one or more of the following reagents: various mAbs (see above); PTX, which inactivates αi-linked G proteins; or MTX, which lacks the enzymatic activity of native PTX (23). PTX and MTX treatment (100 ng/ml) was for 2 h at 37°C and was combined with BCECF-labeling during the final 20 min. Treated cells were washed and used immediately.

Animals. We used adult BALB/c mice (Charles River Laboratories, Wilmington, MA) of both sexes (20–30 g body wt). Mice were housed in a viral antigen–free barrier facility, and kept on sterilized lab chow and water. All experimental procedures comply with National Institutes of Health (Bethesda, MD) guidelines for the care and use of laboratory animals and were approved by the Standing Committees on Animals of Harvard Medical School and The Center for Blood Research.

Subiliac LN Preparation and Intravital Microscopy. Mice were anesthetized by intraperitoneal injection (10 ml/kg) of physiologic saline containing xylazine (1 mg/ml) and ketamine (5 mg/ml). The left subiliac LN was prepared for intravital microscopy as previously described (25). In brief, polyethylene catheters were inserted in the right jugular vein and the left carotid artery. A catheter in the right femoral artery was used for injection of cell suspensions and mAbs. The left subiliac LN was exposed and dissected free of fat tissue. The node was positioned over a microscope slide on a plexiglass stage and kept moist with sterile saline. Sterile vacuum grease and a glass cover slip were applied to enclose the preparation for microscopic viewing. The stage was then placed on an intravital microscope (IV-500; Mikron Instruments, San Diego, CA) equipped with a silicon-intensified target camera (VE1000SIT; Dage mti, Michigan City, IN). The node was visualized by bright field transillumination or epifluorescence from a video-triggered Xenon arc stroboscope (Chadwick Helmuth, El Monte, CA). Video images were recorded using a time base generator (For-A, Montvale, NJ) and a Hi8 VCR (Sony, Boston, MA). Some experiments included injection of FITC-dextran solution (2 mg/ml, 10 ml/kg body wt) after recordings of cell behavior to determine vessel structure, luminal diameter, and venular order. The latter was determined by counting successive generations of branches upstream from the epigastric vein as previously described (25).

Analysis of Endogenous White Blood Cell Behavior. Circulating white blood cells (WBCs) were labeled by intravenous injection of rhodamine 6G (20 mg/kg body wt). This fluorophor stains nuclei and mitochondria. Thus, it allows visualization of myeloid and lymphoid cells as well as (the more faintly labeled) platelets in the circulation, whereas RBCs remain unstained. The distinct nuclear staining patterns of polymorphonuclear (PMNs) and mononuclear leukocytes (MNLs) made it possible to distinguish between these two cell types. An ×100 oil immersion objective with adjustable numerical aperture (Carl Zeiss, Inc., Thornwood, NY) was focused on the upper luminal surface of superficially located HEVs. Using this approach, we determined the nuclear shape of

rolling and sticking cells in the plane of focus. Video analyses performed by different blinded observers yielded essentially identical results, indicating that this method is feasible and reproducible. Between 16 and 83 consecutive rolling cells per venule were categorized as PMNs and MNLs, respectively. Results are expressed as frequency of PMNs and MNLs per 100 identifiable cells that rolled or were stuck (i.e., cells remaining stationary for ⩾30 s) in the field of view. Cells that could not be clearly identified (e.g., because they were out of focus) were excluded.

Parallel to the video recordings, 20 μl blood samples were taken from the retroorbital plexus and diluted in Turk's solution for differential WBC counts on a hemocytometer.

Analysis of BCECF-labeled LNC in PLN-HEVs. Small boluses (10–50 μl) of BCECF-labeled LNCs ($1–2 \times 10^7$ cells/ml) were retrogradely injected via the femoral artery catheter. LNC behavior in PLNs was recorded through ×10 or ×20 water immersion objectives (Achroplan, Carl Zeiss Inc.). Cell behavior in individual vessel segments was determined by playback of video tapes. Cells were considered noninteracting when they moved at the velocity of RBCs, whereas detectably lower velocities were defined as rolling. Cells were considered interacting whether they rolled, arrested, or both. The rolling fraction is the percentage of cells that interact with a given venule in the total number of cells that enter that venule during the same period. The sticking fraction is the percentage of interacting cells that become immobile for ⩾30 s. In some experiments, sticking LNCs that accumulated in PLN venules during the 10-min period after intraarterial bolus injection of 10^7 LNCs were counted. LNC accumulation was expressed as number of sticking cells per mm^2 of lumenal surface area (calculated from venular diameter and length assuming cylindrical geometry). A PC-based image analysis system (26) was used to measure velocities of ⩾15 consecutive rolling and 20 noninteracting LNCs before and after treatment with mAbs, PTX, or MTX in one representative venule per animal. Data were used to determine mean fast cell velocity (V_{fast}), centerline velocity, mean blood flow velocity (V_{blood}), wall shear rate, and rolling velocity (V_{roll}) as previously described (25). To correct for the influence of varying V_{blood} on rolling, the relative rolling velocity (V_{rel}) was also calculated according to the following formula: $V_{rel} = V_{roll}/V_{blood} \times 100\%$. V_{roll} data from different experiments were pooled to compare treatment effects on V_{roll} histograms, a sensitive indicator of the strength of rolling interactions.

Statistical Methods. Data in graphs and tables are shown as mean ± SD, unless otherwise indicated. For statistical comparison of two samples, a two-tailed Student's *t* test was used when applicable. Multiple comparisons were performed employing the Kruskal-Wallis test and Bonferoni correction of *P*. Velocity histograms were compared using the Mann-Whitney U-test and the Kolmogorov-Smirnov test. Differences were considered statistically significant when $P < 0.05$.

Results

Endogenous Leukocyte Behavior in Subiliac PLNs. Nuclei of endogenous WBCs were labeled with rhodamine 6G to study the behavior of PMNs and MNLs in subiliac PLNs (Fig. 1). In agreement with studies of other organs, we observed heterogeneous adhesive behavior in venules, whereas arterioles or capillaries did not support interactions. High-power microscopy of superficial HEV segments allowed us to distinguish rolling and/or sticking MNLs and PMNs in the plane of focus. Thus, although some cells could not be categorized when they were out of focus, it was possible to determine the relative frequency of subset behavior. Of all the identifiable rolling WBCs in HEVs (300 cells in 7 HEVs of 3 animals) the frequency of MNLs was 30%; the remainder (70%) were PMNs. The proportion of PMNs in the rolling population was somewhat higher than their frequency in systemic blood (Fig. 2); differential blood counts showed that 44 and 56% of circulating WBCs were PMNs

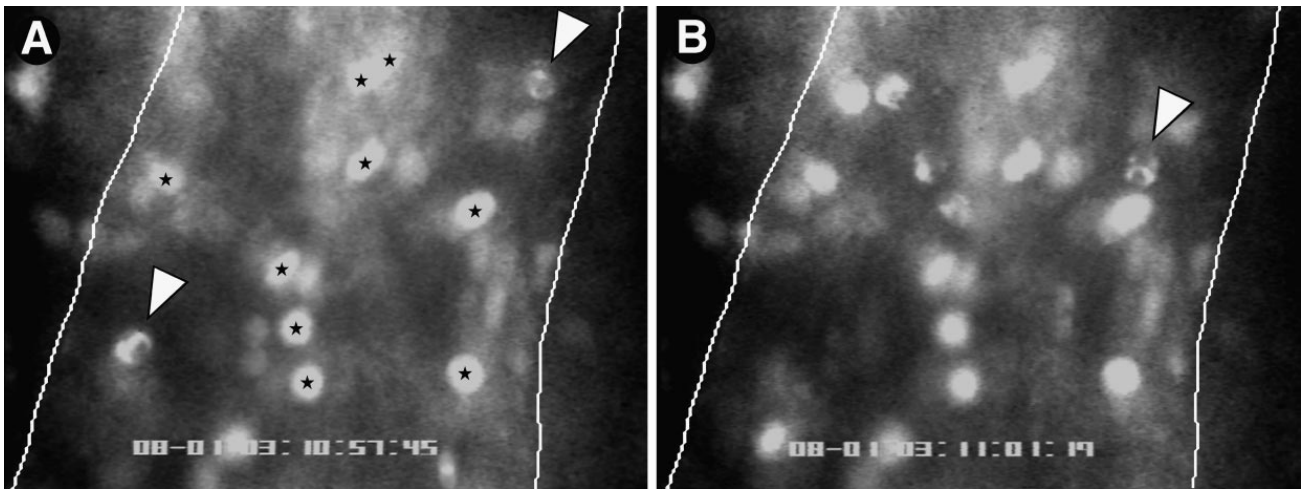

Figure 1. Both PMNs and MNLs roll, but only MNLs stick in PLN-HEVs. Endogenous circulating WBCs were labeled in situ with the nuclear dye rhodamine 6G. Cells were recorded by fluorescence microscopy through an ×100 objective during their passage through HEVs. The micrographs show typical scenes in a segment of an order III venule (50-μm diameter, blood flow from top to bottom). Lines were drawn to demarcate lateral borders of the lumenal compartment. WBCs in the plane of focus show two distinct nuclear staining patterns allowing the identification of PMNs (*irregular shape*) and MNLs (*homogenous round or oval staining pattern*). (*A*) Two rolling PMNs (*arrows*) and several sticking MNLs (*stars*) can be seen. (*B*) 3.7 s later, one of the PMNs (*A*, *lower left*) has rolled out of the field of view, whereas the other PMN (*arrowhead*) has continued to roll slowly through the vascular segment. Sticking MNLs did not change their position. In the meantime, several additional rolling PMNs and MNLs entered the field of view.

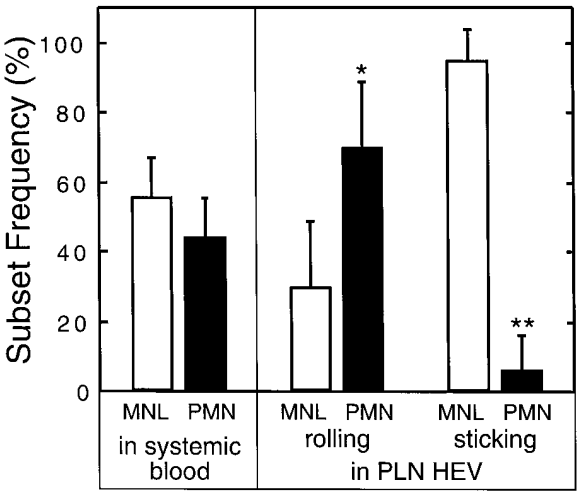

Figure 2. Frequency of rolling and sticking MNLs and PMNs in non-inflamed PLN-HEVs. Nuclei of circulating WBCs were fluorescently labeled by intravenous injection of rhodamine 6G. Differential counts of PMNs and MNLs in systemic blood were determined in parallel to video recordings of WBC behavior in PLN-HEVs. The frequency of PMNs and MNLs in the total flux of identifiable rolling cells (16–83 consecutive rolling cells in 7 HEVs of 3 separate preparations) was determined. 10 HEVs in 3 preparations were scanned to determine the frequency of sticking cell subsets (i.e., cells that did not move during a 30 s time period). *$P < 0.01$; **$P < 0.001$ versus MNL (Student's *t* test).

and MNLs, respectively (the frequency of PMNs is slightly elevated over normal levels for mice, and most likely reflects release of neutrophils from the marginating pool due to surgical trauma). We conclude that the ability to tether and roll within HEVs is not specific for lymphocytes, but is shared by other leukocyte subsets, including neutrophils.

A subpopulation of initially rolling cells eventually arrested, adhering firmly. This behavior was almost exclusively limited to MNLs, whereas PMNs continued to roll and, eventually, detached from the vessel wall. Indeed, 23.2 ± 8.9% (mean ± SD) of rolling MNLs became stuck during their observable passage through HEVs, whereas only 0.5 ± 0.6% of PMNs displayed this behavior (data not shown). Similarly, a survey of firmly adherent cells (i.e., cells that were already stuck when the recording was started and did not move for at least 30 s thereafter) in HEVs revealed that nearly all of these cells were MNLs as well (10 HEVs in 3 animals).

Behavior of Adoptively Transferred LNCs in PLN-HEVs. Although in situ staining of WBCs permitted the differentiation of the nuclear shape of rolling cells in segments of some HEVs, rhodamine 6G labeling did not allow us to perform a selective and quantitative analysis of lymphocyte behavior in the entire PLN microcirculation. Therefore, we assessed the adhesive behavior of pooled lymphocytes that were isolated from peripheral and mesenteric nodes and stained in vitro with the intracellular fluorophor BCECF. Labeled LNCs were retrogradely injected through the right femoral artery and observed during their passage through the left subiliac PLN.

LNC interactions mirrored the behavior of the endogenous MNLs described above. A fraction (~30% on average) of LNCs did not interact with the venular walls, but the majority of cells rolled, especially in higher order venules. A small fraction of cells exhibited either multiple interactive behaviors (e.g., momentary stops or hesitations, skipping, variable rolling speeds) or transient arrest and release (preceded and/or followed by rolling). A significant number of rolling LNCs (up to 30% in some HEVs) subsequently became firmly adherent. Less than 1% became stationary immediately upon entry into HEVs, a site where microvascular hemodynamics and endothelial cell properties may change abruptly.

In contrast to rhodamine 6G staining of WBCs, which requires high magnification for reliable detection of cells, BCECF-labeling confers significant brightness and, therefore, allows visualization of labeled cells at lower magnification (×10 objective) and within a larger field of view. This permits parallel evaluation of LNC behavior within different segments of the nodal venular tree. A recent analysis of the microvascular anatomy of murine subiliac PLNs has shown that up to five branching orders can be identified in a typical venular tree (25). One (or more) order I venule is located in the hilus of subiliac PLNs and drains into a branch of the extralymphoid superficial epigastric vein. Order I venules are formed by the merging of smaller collecting venules (order II) in the nodal medulla that collect blood from higher order postcapillary venules (orders III–V) in the sub- and paracortex. To determine if there are segmental differences in lymphocyte recruitment, we correlated rolling and sticking fractions, as well as the accumulation of sticking LNCs, with the venular order (Fig. 3 *A*). In agreement with previous studies using L-selectin–transfected lymphoma cells (25), we found that LNCs were able to attach and roll in all venules draining the node proper, but rolling fractions were significantly larger in higher order venules (Fig. 3 *B*). Likewise, arresting cells were much more frequently observed in the highest order venules (Fig. 3 *C*). The paracortical orders III–V HEVs also supported the majority of long-term sticking, resulting in the preferential accumulation of LNCs in these venular segments (Fig. 3 *D*). A significant number of HEVs were noted whose lumen widened abruptly where several capillaries converged in the paracortex. This transition results in an immediate slowing of cells, and may lead to a local disruption of smooth blood flow, which in turn may aid in promoting lymphocyte–HEV interactions. It was primarily at these sites that rare lymphocytes became stuck without discernible rolling preceding the arrest.

Lymphocyte Adhesion in PLN Venules Is L-selectin–dependent. To investigate the contribution of L-selectin to localization of lymphocytes in PLNs, we pretreated LNCs with Mel-14, a function-blocking anti–murine L-selectin mAb. The antibody effect was strikingly complete, inhibiting nearly all interactions of labeled LNCs with the PLN vasculature (Fig. 4). This differs significantly from previous intravital microscopy studies in murine PPs, in which anti–L-selectin only partially reduced interacting fractions (11, 13). In this site, the integrin α4β7 can also contribute to lymphocyte tethering and rolling. Thus, we tested whether

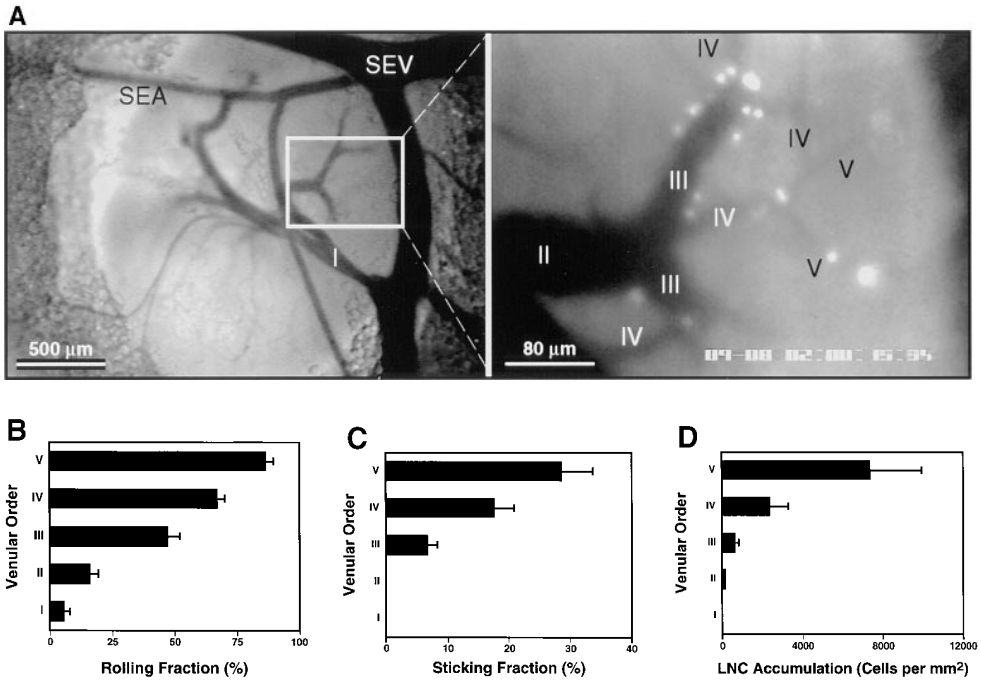

Figure 3. Lymphocyte interactions in the nodal venular tree are spatially restricted. (*A*) Micrographs show a typical subiliac LN preparation at low (×4 objective, *left*) and high (×20 objective, *right*) magnification. The panel on the left shows the LN embedded in fatty tissue and partially covered by the superficial epigastric artery (*SEA*) and vein (*SEV*). Venous blood from the LN drains into an extralymphoid side branch of the SEV via a large order I venule in the nodal medulla (*I* in left panel). An area of the PLN (*rectangle* on left) containing some of the tributaries (orders II–V) to this collecting venule is shown on the right 30 min after injection of BCECF-labeled LNCs (some cells appear larger because of bleeding of the bright fluorescence signal and/or because they are out of focus). Interacting LNCs are preferentially found in high-order HEV, and rarely stick in order I or II venules. (*B*) Rolling fractions and (*C*) sticking fractions of BCECF-labeled LNCs in PLN venules were correlated with venular order. LNCs were retrogradely injected into the right femoral artery, and their rolling and sticking behavior during their initial passage through the LN was analyzed as described in Materials and Methods. Data shown are means ± SEM of 9 experiments (4–10 venules each). (*D*) LNC accumulation (10 min after injection of 10^7 cells) in a representative subiliac LN preparation. Bars depict mean ± SD of accumulated LNCs in a total of 67 venules.

integrins were similarly able to support LNC rolling in PLNs. No significant effect on the frequency of rolling was found with neutralizing antibodies to LFA-1 or α4 integrins.

The Strength of LNC Rolling Interactions Is Integrin- and G Protein–independent. The α4β7 integrin component of LNC rolling in PPs was found to strengthen rolling interactions and to reduce lymphocyte rolling velocity (11, 13). We asked whether there might be a similarly significant contribution by α4 or LFA-1 integrins to the strength of LNC rolling interactions in PLNs. To address this question, we compared microvascular hemodynamics and V_{roll} histograms by measuring velocities of at least 35 consecutive (⩾15 rolling and ⩾20 noninteracting) cells in typical order III HEV before and after antibody treatment (Table 1). Video analysis allowed us to make precise comparisons of V_{roll} within the same vessels before and after mAb treatment (Fig. 5, *A* and *B*). No significant mAb effect could be ascertained.

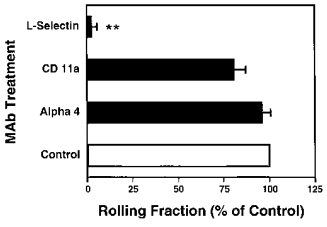

Figure 4. Lymphocyte rolling in PLNs is L-selectin–dependent. LNCs rolling fractions were analyzed before (control) and after treatment of cells and animals with blocking mAbs (α4, mAb PS/2; LFA-1, mAb Tib 213; L-selectin, mAb Mel-14). Bars depict rolling fractions as percentage of control cell rolling in the same venule; data shown are mean ± SEM of rolling fractions from 3–5 experiments of 4–10 vessels each. $^{**}P < 0.001$ versus all groups (Kruskal Wallis test with Bonferoni correction).

Since $G\alpha_i$-linked signaling pathways are known to be involved in physiologic integrin activation and lymphocyte homing to PLNs, we also measured the V_{roll} of LNCs in which these signaling molecules had been blocked by pretreatment with PTX. Excluding those cells that arrested, there was no significant difference between V_{roll} profiles of LNCs treated with functionally active PTX or the inactive mutant form, MTX, or with untreated cells (Fig. 5 *C* and data not shown).

LFA-1 Mediates Firm Adherence of Lymphocytes in PLN-HEVs. Isolated LNCs and recipient mice were pretreated with anti-CD11a antibody to block LFA-1–dependent adhesion, and cell behavior was observed within subiliac PLNs. The mAb treatment essentially abrogated LNC sticking in all venular orders (Fig. 6). Importantly, sticking was also abolished when LNC rolling was blocked by treatment with anti–L-selectin mAb Mel-14, even when LFA-1 function was not blocked. Treatment with either anti–L-selectin or anti–LFA-1 also eliminated the behavior of the small subset of LNCs that seemed to arrest immediately upon entry into HEVs, without discernible rolling (data not shown). In contrast, anti-α4 integrin antibody had no statistically significant effect on LNC sticking.

Rolling Lymphocytes Require Rapid $G\alpha_i$-linked Signaling to Trigger Sticking in PLN-HEVs. Our findings strongly suggest that LFA-1 is responsible for firm LNC arrest, but not

Table 1. *Venular Microhemodynamics and Rolling Velocities of LNCs*

mAb inhibition	No. Venules/ No. animals	Diameter	V_{fast}	V_{blood}	WSR (WSS)	V_{roll} (Median)	V_{rel} (Median)
		μm	$\mu m/s$	$\mu m/s$	s^{-1} (dyne/cm^2)	$\mu m/s$	%
Control	3/3	38.4 ± 5.9	1236 ± 603	1105 ± 456	228 ± 75 (5.6 ± 1.9)	38.6 ± 21.7 (14.7)	3.4 ± 2.8 (2.0)
L-selectin	3/3	38.4 ± 5.9	1099 ± 266	1168 ± 486	250 ± 59 (6.3 ± 1.5)	N/A	N/A
Control	4/4	36.2 ± 8.5	999 ± 521	1150 ± 309	267 ± 82 (6.7 ± 2.1)	24.2 ± 18.6 (10.0)	2.7 ± 1.8 (0.9)
α4 integrin	4/4	26.2 ± 8.5	1456 ± 673	1297 ± 475	289 ± 70 (7.2 ± 1.7)	34.1 ± 29.5 (15.8)	2.7 ± 2.7 (1.3)
Control	3/3	32.7 ± 4.8	1103 ± 482	1021 ± 386	248 ± 71 (6.2 ± 1.8)	43.0 ± 34.9 (32.1)	4.5 ± 4.0 (3.5)
LFA-1	3/3	32.7 ± 4.8	1109 ± 462	1149 ± 492	273 ± 81 (6.8 ± 2.0)	44.9 ± 37.6 (30.8)	4.4 ± 3.8 (2.6)
MTX	3/3	36.9 ± 5.0	1592 ± 815	1392 ± 949	319 ± 91 (8.0 ± 2.3)	64.1 ± 40.4 (23.2)	4.9 ± 3.7 (1.4)
PTX	3/3	36.9 ± 5.0	1792 ± 809	1569 ± 662	332 ± 99 (8.3 ± 2.5)	66.4 ± 48.6 (33.9)	5.2 ± 5.0 (1.9)

Mean velocities of noninteracting (V_{fast}) and rolling (V_{roll}) LNCs in one representative order III venule per animal were measured. These data together with the venular diameter were used to calculate V_{blood} and wall shear rate (WSR) as described in Materials and Methods. The wall shear stress (WSS) was estimated based on the assumption that the blood viscosity in HEVs is 0.025 Poise. To correct for hemodynamic differences between control and teatment periods in individual venules that may have mechanically affected LNC rolling behavior, V_{roll} was also expressed as percentage of V_{fast} (V_{rel}). Anti–L-selectin treatment essentially eliminated LNC rolling in HEVs. Thus, no data for V_{roll} and V_{rel} were obtainable. Data shown are mean ± SD. Since velocity histograms of V_{roll} indicate that data were not normally distributed (see Fig. 5), median values are shown as well.

for initial rolling interactions. This integrin is known to require cell activation signals to become functional (27). Thus, it seemed likely that a selective activation event was operating to mediate the transition from L-selectin– to LFA-1–dependent adhesion in rolling LNCs. We tested the hypothesis that this activation step involved PTX-sensitive signaling pathway(s). The effect of PTX treatment was similar to that of anti-CD11a, in that LNCs were able to attach and roll normally in PLN-HEVs (Fig. 7 *A*), but were unable to arrest (Fig. 7 *B*). In contrast, mutant inactive PTX

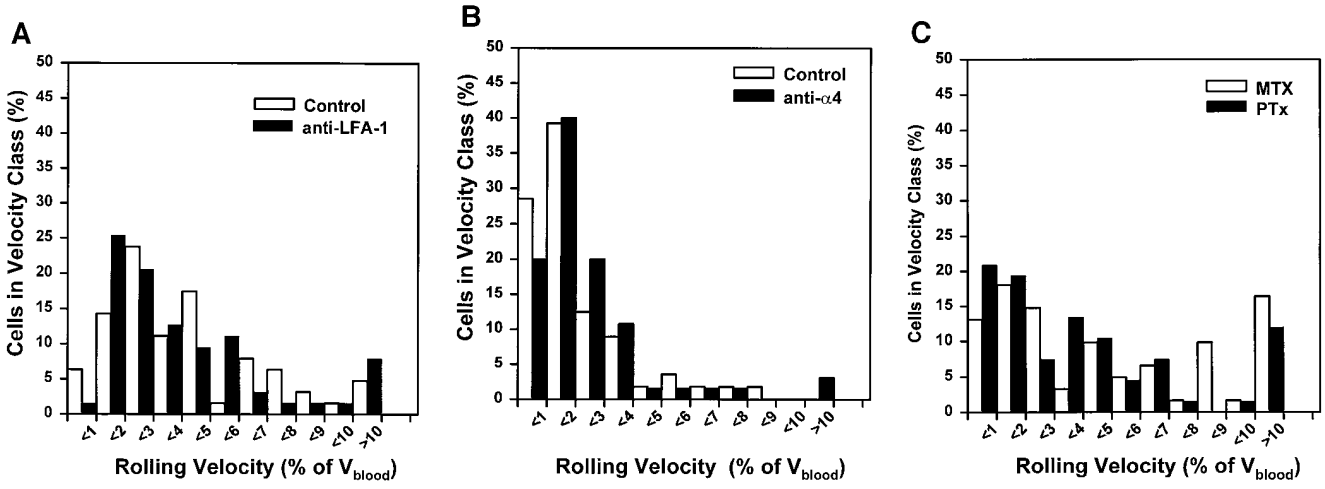

Figure 5. The strength of LNC rolling in HEVs is not augmented by α4 or LFA-1 integrins, and is not PTX sensitive. Frequency histograms were generated by measuring rolling velocities of individual LNCs in order III venules before (control) and after treatment with (*A*) anti–LFA-1, (*B*) anti-α4, or (*C*) PTX or MTX. V_{roll}, V_{fast}, and V_{blood} were determined in the same vessels before and after mAb, MTX, or PTX treatment as described in Materials and Methods (results of hemodynamic measurements are given in Table 1). To account for hemodynamic differences between control and treatment period, V_{rel} was calculated as percentage of V_{blood}. Frequency distributions were calculated after cells were assigned to velocity classes with V_{rel} >0% to <1%, 1% to <2%, and so on. Statistical comparison of population means and distributions revealed no significant differences between rolling velocities (P >0.05).

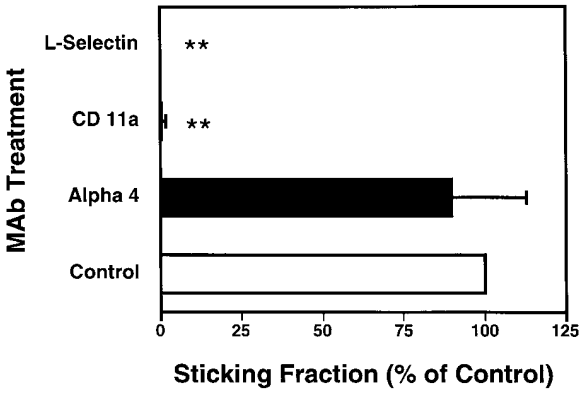

Figure 6. Lymphocyte sticking in PLN-HEVs is mediated by LFA-1. The fraction of rolling LNCs that became stuck for ⩾30 s was determined before (control) and after treatment of cells and animals with blocking mAbs (α4, mAb PS/2; LFA-1, mAb Tib 213; L-selectin, mAb Mel-14). Bars depict sticking fractions as percentage of control cell sticking in the same venule; data shown are mean ± SEM of sticking fractions from 3–5 experiments (4–10 venules each). $^{**}P < 0.001$ versus α4 and control group (Kruskal Wallis test with Bonferoni correction).

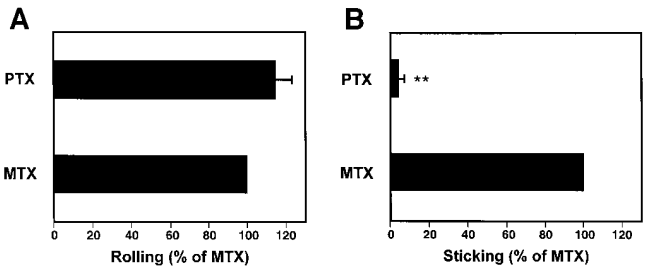

Figure 7. Sticking of LNCs in PLN-HEV, but not rolling, is blocked by PTX. To test the role of $G\alpha_i$-linked proteins, LNCs were treated with PTX or the inactive mutant form, MTX, as a control. Cells were labeled with BCECF and injected into the feeding artery of a subiliac PLN. (*A*) Rolling and (*B*) sticking fractions of treated LNCs in subiliac LN venules were determined. Data are shown as mean ± SEM of 3 experiments (5–10 venules each). $^{**}P < 0.001$ (Student's *t* test).

(MTX) did not inhibit LNC sticking. The mutant form of PTX contains two amino acid substitutions ($Arg^9 \rightarrow Lys$ and $Glu^{129} \rightarrow Gly$) and retains the ability to interact with cell membranes, but lacks the enzymatic ability to ADP-ribosylate α_i subunits of heterotrimeric G proteins (23). Thus, it seems likely that the blockade of sticking by PTX was due to inactivation of G protein–linked signaling, and not due to intrinsic surface modifications and/or steric hindrance of requisite surface molecules.

Discussion

We have examined the interactions of blood-borne leukocytes with PLN-HEVs in order to dissect the molecular mechanisms of lymphocyte homing to PLNs. The experimental data suggest that an organ-specific adhesion cascade operates within resting PLNs that is selective for and efficient in recruiting naive lymphocytes, while excluding myeloid cells or lymphocyte populations that express little or no L-selectin (Fig. 8). Although L-selectin mediates attachment and rolling interactions in PLN-HEVs, LFA-1 was required for subsequent lymphocyte sticking. Adhesion via LFA-1, but not L-selectin, was inhibited by PTX, indicating that heterotrimeric G protein signaling is required for affinity upregulation of LFA-1. This cascade of molecular-adhesive events in PLNs is similar to, but molecularly distinct from, those previously characterized for lymphocyte homing to PPs and intestinal lamina propria, and for granulocyte accumulation in other organs (11, 28, 29).

Previous ultrastructural and histologic studies of the PLN subcortex and medulla have suggested that lymphocyte extravasation may occur preferentially within paracortical venules that feature specialized luminal morphology. These postcapillary vessels (corresponding to order IV and V venules in subiliac LNs) are lined by high cuboidal endothelial cells. Further downstream, endothelial cells are arranged in an overlapping plate pattern followed by a smooth layer of flat endothelial cells that is indistinguishable from nonlymphoid microvessels (corresponding to the lining of order I and II venules; references 1, 30, 31). The counter-receptors for L-selectin and LFA-1 are found in abundance on the luminal surface of postcapillary HEVs, and in particular on ridgelike structures that may further facilitate or reinforce cellular interactions (32, 33). Our results provide a functional correlate for these morphologic observations: leuko-

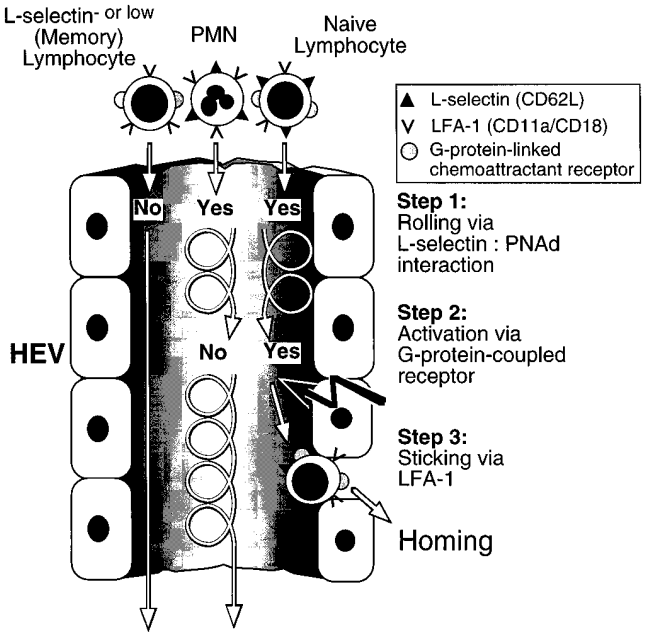

Figure 8. Homing to PLN is mediated by a unique cascade of molecular adhesive and signaling events. At least three distinct steps must occur for lymphocyte homing via HEVs. Only cells that express L-selectin at sufficient density can tether and roll via binding to PNAd (*Step 1*). Most lymphocytes (such as subsets of activated/memory cells) that express little or no L-selectin pass HEVs without interacting. Subsequently, rolling cells must encounter a $G\alpha_i$-linked activating stimulus (*Step 2*) which triggers functional upregulation of LFA-1 (*Step 3*). Rolling PMNs cannot respond to this lymphocyte-specific chemoattractant signal. The unique combination of these consecutive steps results in the highly efficient and selective recruitment of preferentially naive lymphocytes.

cyte rolling and lymphocyte sticking were spatially regulated, occurring preferentially in high order subcortical venules. Thus, our studies confirm those of Marchesi and Gowans who proposed over 30 years ago that lymphocyte homing is a unique feature of HEV in the nodal paracortex (31).

Early experiments in mice demonstrated the inhibition of lymphocyte homing to PLNs by treatment with mAb Mel-14 to murine L-selectin and thus L-selectin has been dubbed the lymphocyte homing receptor (14). In addition to its well-known function as a mediator of leukocyte rolling, recent studies have shown that L-selectin ligation can induce intracellular signaling events (34, 35) and that extensive antibody- or ligand-induced cross-linking of L-selectin can trigger functional upregulation of β2 integrins in neutrophils and lymphocytes (36, 37). Our analysis of LNCs and endogenous leukocyte behavior demonstrates that L-selectin is both necessary and sufficient for tethering and rolling of LNCs in all venular orders, but suggests that L-selectin engagement alone is insufficient to induce sticking.

On rolling cells, L-selectin engagement is presumably brief and restricted to the small fraction of total L-selectin molecules within the area of contact with the vessel wall. Our results show that L-selectin–mediated rolling of PMNs in HEVs was rarely followed by sticking, and a detailed analysis of V_{roll}s suggests that the strength of LNC rolling interactions was not influenced by LFA-1 or α4 integrins. Moreover, L-selectin signaling has been reported to be insensitive to PTX (34), whereas LNC sticking in HEVs was essentially abrogated by PTX pretreatment. Thus, L-selectin signaling, if it occurs during lymphocyte–HEV interactions, does not appear sufficient to mediate arrest or alter rolling through integrin activation. However, our studies do not exclude the possibility that L-selectin signaling may synergize with other activation pathways that involve PTX-sensitive G proteins.

Lymphocytes from noninflamed lymph nodes are primarily naive T and B cells that are characteristically L-selectin^{hi}, LFA-1^{+}, and α4^{lo} (38, 39). Consistent with this specialized array of surface adhesion molecules, naive lymphocytes are the predominant subset that enters PLNs via HEVs (39, 40). The finding that LNC accumulation in murine PLNs is dependent on L-selectin implies that lymphocytes that do not express L-selectin, or express only low levels, may be excluded from homing to PLNs because they cannot tether and roll along the vessel wall. L-selectin^{low} lymphocyte populations may include many recently activated cells as well as a sizable fraction (~30%) of circulating memory cells (38, 39). On the other hand, these results suggest that, unless precluded by the existence of naive cell-specific activating factors, memory cell subsets that express L-selectin and LFA-1 should be capable of homing to PLNs via the HEV route. Indeed, recent short-term homing studies of splenic memory T cell subsets indicate that a significant number of memory cells retain a significant capacity to home via PLN-HEVs in mice (39).

The concept that L-selectin is essential for lymphocyte traffic to PLNs is also in agreement with the phenotype of L-selectin–deficient mice, which display an ~90% reduction in the size and cellularity of PLNs due to a greatly reduced influx of lymphocytes via HEV (12, 16–18). The majority of resident lymphocytes in the PLNs of these animals display a memory phenotype, and it has been proposed that these cells arrive in PLNs predominantly via afferent lymph vessels (18). However, it is possible that some L-selectin–deficient cells may reach PLNs after adhering to HEVs through an alternative pathway. We have previously shown that circulating activated platelets can bridge between L-selectin deficient lymphocytes and HEVs because platelet P-selectin mediates platelet tethering to both P-selectin glycoprotein ligand 1 (PSGL-1) on lymphocytes and PNAd on HEVs (41, 42). Consistent with this idea, we have previously shown that the rolling of endogenous WBCs in wild-type mice was not completely inhibitable by anti–L-selectin mAb (41). Moreover, ~10% of the WBCs that passed through PLNs in L-selectin–deficient mice rolled in HEVs (42). The fact that LNCs did not display L-selectin–independent rolling in our experiments does not contradict this platelet delivery concept. It is unlikely that LNCs had significant numbers of platelets on their surface because they were directly isolated from LNs and washed extensively before injection, and LNC behavior was only analyzed for a short time (seconds to minutes) after intraarterial injection. This period may not have been sufficient to allow significant association with activated platelets which may be infrequently encountered in the blood stream.

Lymphocyte homing to PLNs in LFA-1–deficient mice has not been directly examined as yet. However, PLNs in these mice are reportedly smaller than those of wild-type littermates (20). Moreover, it has been reported that although systemically-induced delayed type hypersensitivity responses are apparently normal in the absence of LFA-1 (43), recall responses to cutaneously applied antigen are severely impaired in LFA-1–deficient mice (20). This phenotype is similar to that of L-selectin–deficient mice in which an inability to mount a cutaneous hypersensitivity response was shown to be due to the lack of naive lymphocyte homing to the draining PLNs where cutaneous antigens are presented (16, 17). Our findings demonstrating LFA-1 involvement in lymphocyte arrest in PLN–HEVs may provide an explanation for these observations, suggesting that the inefficient cutaneous response in LFA-1–deficient mice may reflect a defect in normal sensitization of lymphocytes within PLNs.

LFA-1 exists in an inactive state on resting LNCs, but its ligand binding activity may be rapidly modulated by a variety of mechanisms (27, 44–46). In addition to L-selectin cross-linking (discussed above), several distinct signaling pathways have been implicated in β2 integrin activation, including ligation of lymphocyte antigen receptors and chemoattractant receptors that signal through heterotrimeric G proteins. The latter include receptors for physiologic chemoattractants such as chemokines, a class of receptors whose signaling is both rapid and sensitive to inactivation by PTX (46, 47).

We found that LFA-1–dependent firm adhesion of LNCs in PLN-HEVs was PTX-sensitive, analogous to prior

studies of LNC homing to PPs (9, 11). However, the PTX-induced inhibition of LNC sticking in PPs was reversible by LNC activation with PMA, a phorbol ester that directly activates protein kinase C (9). We attempted but were unable to circumvent the effects of PTX inhibition on LNC sticking in PLN-HEVs by PMA pretreatment of LNCs before injection. PMA has been shown to upregulate the affinity of leukocyte integrins, including LFA-1 (48) and $\alpha4\beta7$ (49), but PMA treatment also causes rapid shedding of L-selectin and resulted in a dramatic reduction in LNC rolling in PLN-HEVs (reference 50 and data not shown). We performed additional in vitro studies using a parallel plate flow chamber (41) and affinity-isolated PNAd and intercellular adhesion molecule (ICAM)–1, endothelial ligands for L-selectin and LFA-1, respectively. PMA induced equivalent sticking of both PTX and mutant toxin–treated LNCs to ICAM-1 under static conditions or at low shear (1.6 dyne/cm^2) within a narrow temporal window (4.5–6 min after activation, our unpublished observation). Surface-expressed L-selectin was concomitantly downregulated, resulting in a failure of most cells to tether to the coated substrate at higher shear rates or at later time points. In contrast to PLNs, primary adhesion of LNCs in PPs can be alternatively mediated by either L-selectin or $\alpha4\beta7$ (11). Thus, the ability of PMA-activated, PTX-treated LNCs to stick in PP-HEVs, but not PLN-HEVs, was most likely due to the differential contribution by $\alpha4\beta7$ to primary adhesion and may also have resulted in more efficient sticking in PP-HEVs afforded by the synergy of activated $\alpha4\beta7$ and LFA-1.

Taken together, our results suggest that rolling lymphocytes are activated in PLN-HEVs by one or more potent adhesion-triggering chemoattractant(s) that exert their effect via $G\alpha_i$-coupled lymphocyte surface receptor(s). Our observations suggest that unless one postulates signals occurring before lymphocyte entry into HEVs, the signaling event must be capable of triggering LFA-1 in less than 1 s. Interestingly, we noted LNCs to be extraordinarily sensitive to temperature effects: LNC preparations that were not carefully kept at 37°C before intraarterial injection rolled normally in HEVs, but were incapable of sticking during their initial passage through HEVs (our unpublished observation). This indicates that the efficient detection and processing of the chemoattractant signal and/or the subsequent integrin response are critically dependent on unperturbed cellular metabolism. While the identity of the lymphocyte chemoattractant(s) in PLN-HEVs remain(s) to be determined, our findings do not exclude the possibility that signals which upregulate LFA-1 affinity may be sufficient for arrest, but insufficient for subsequent diapedesis.

Our results imply that the recruitment of (mostly naive) lymphocytes to PLNs is also controlled in part by a selective ability to recognize specific chemoattractant(s). Nearly all granulocytes and 70–80% of all circulating lymphocytes (constituting the majority of MNLs) express L-selectin (51). The observation that rolling PMNs in PLN-HEVs were slightly more frequent than MNLs when compared to their respective frequency in the blood stream is consistent with the differential prevalence of L-selectin$^+$ cells in the two subsets. However, as originally noted by Lewinsohn et al., the distinction between granulocyte and lymphocyte recruitment to PLNs is not based on differential engagement of the homing receptor L-selectin (51). Although both PMNs and MNLs are known to express LFA-1 in an inactive or low-affinity conformation (27), we observed that endogenous MNLs, but not PMNs, could firmly arrest in PLN-HEVs. This implies that the HEV-specific activation signal was selectively detected by rolling lymphocytes, but not by myeloid cells. Though variations in homing receptor expression reflect differentiation of lymphocyte subpopulations (and critically impact recirculatory routes), the possible role that chemoattractants may play in regulating subpopulation homing (e.g., naive versus memory lymphocytes) remains to be determined.

The data presented here describe lymphocyte homing to PLNs as similar to, but distinct from, the multi-step adhesion cascade in PPs, which requires lymphocyte $\alpha4\beta7$ interaction with endothelial MAdCAM-1. In this site, $\alpha4\beta7$ plays a critical bridging role, slowing the L-selectin–initiated rolling of cells sufficiently to allow LFA-1 engagement. In addition, $\alpha4\beta7$ can also mediate tethering (albeit less efficiently than L-selectin), thus allowing some lymphocytes to home to PPs in an L-selectin–independent manner. Indeed, although anti–L-selectin greatly reduced the total leukocyte rolling flux in PP-HEVs (65–90%), the fraction of lymphocytes that entered PP-HEVs and subsequently became stuck was reduced by only 35% (11, 13). Although lymphocyte homing to rat PLNs has been reported to involve $\alpha4$ integrins, and expression of the $\alpha4$ integrin ligand VCAM-1 has been found in rat PLN-HEVs (52), most HEVs in uninflamed adult murine and human PLNs were reported to express little, if any, MAdCAM-1 or vascular cell adhesion molecule 1 (VCAM-1; 53–55). This is consistent with our present findings and with earlier homing studies using anti-$\alpha4$ mAbs or $\beta7$-deficient animals (13, 56, 57).

The apparent lack of a requisite bridging adhesive interaction between L-selectin and $\beta2$ integrin engagement in PLNs may reflect the much higher density of L-selectin ligands on PLN-HEVs, which alone may allow sufficiently strong and slow rolling interactions (15). Our analysis of hemodynamic parameters presented here and in an earlier report (25) indicate that, on average, V_{blood} (1.1 ± 0.5 mm/s versus 3.2 ± 0.2 mm/s) and WSR (228 ± 75 s^{-1} versus 418 ± 39 s^{-1}) are significantly lower in PLN venules than those encountered in PP-HEVs (58), yet the V_{roll} is similar (11, 58). Although the requirement for $\alpha4\beta7$ in PP homing may reflect the greater need for strengthened rolling adhesions to allow sufficient slowing for LFA-1 engagement, the dissimilar requirements of PLN and PP homing clearly provide a mechanism for the differential recruitment of compartmentalized lymphocyte subsets (39).

However, our results do not formally exclude the existence of additional intermediate adhesive interactions in PLNs. In addition to the platelet delivery mechanism (discussed above), a number of other receptors have been implicated in PLN homing, such as the hyaluronate receptor CD44 and the mucin CD43 on lymphocytes, and vascular adhe-

sion protein 1 (VAP-1) expressed on human PLN-HEVs (59–61). On the other hand, the strikingly complete inhibition of LNC rolling and sticking by mAbs to L-selectin and LFA-1, respectively, suggests that any additional molecular adhesive pathways (other than platelet P-selectin) are unable to confer detectable mechanical stability to either of these events under the experimental conditions employed here.

In conclusion, we have demonstrated a unique adhesion cascade mediating lymphocyte homing to PLN-HEVs. We have confirmed the site of lymphocyte adhesion in PLNs as high-order subcortical post-capillary venules, and have refined the understanding of leukocyte adhesive behavior therein. The critical roles of L-selectin for attachment and rolling and affinity-upregulated LFA-1 for firm adhesion in normal lymph nodes have profound implications for the recirculatory routes of naive and memory lymphocyte populations, and illustrate the singular role that chemoattractant signals play in recruiting or excluding leukocyte subsets from specialized tissues.

We wish to thank Guiying Cheng and Brian Fors for outstanding technical support, Dr. Rino Rappuoli for providing MTX, and Jay Mizgerd for critical reading of the manuscript.

This study was supported by National Institutes of Health grants HL-54936 and HL-56949 (to U.H. von Andrian), and GM-37734 and AI-37832 (to E.C. Butcher).

Address correspondence to Dr. Ulrich H. von Andrian, The Center for Blood Research, 200 Longwood Ave., Boston, MA 02115. Phone: 617-278-3130; Fax: 617-278-3190; E-mail: uva@cbr.med.harvard.edu

Received for publication 18 August 1997 and in revised form 19 November 1997.

References

1. Gowans, J.L., and E.J. Knight. 1964. The route of re-circulation of lymphocytes in the rat. *Proc. R. Soc. Lond. B. Biol.* 159:257–282.
2. Butcher, E.C., R.G. Scollay, and I.L. Weissman. 1980. Organ specificity of lymphocyte migration: mediation by highly selective lymphocyte interaction with organ-specific determinants on high endothelial venules. *Eur. J. Immunol.* 10:556–561.
3. Butcher, E.C., and L.J. Picker. 1996. Lymphocyte homing and homeostasis. *Science*. 272:60–66.
4. Butcher, E.C. 1991. Leukocyte-endothelial cell recognition: three (or more) steps to specificity and diversity. *Cell*. 67: 1033–1036.
5. Shimizu, Y., W. Newman, Y. Tanaka, and S. Shaw. 1992. Lymphocyte interactions with endothelial cells. *Immunol. Today*. 13:106–112.
6. Springer, T.A. 1994. Traffic signals for lymphocyte recirculation and leukocyte emigration: the multi-step paradigm. *Cell*. 76:301–314.
7. von Andrian, U.H., J.D. Chambers, L.M. McEvoy, R.F. Bargatze, K.E. Arfors, and E.C. Butcher. 1991. Two-step model of leukocyte–endothelial cell interaction in inflammation: distinct roles for LECAM-1 and the leukocyte β_2 integrins *in vivo*. *Proc. Natl. Acad. Sci. USA*. 88:7538–7542.
8. Lawrence, M.B., and T.A. Springer. 1991. Leukocytes roll on a selectin at physiologic flow rates: distinction from and prerequisite for adhesion through integrins. *Cell*. 65:859–873.
9. Bargatze, R.F., and E.C. Butcher. 1993. Rapid G protein–regulated activation event involved in lymphocyte binding to high endothelial venules. *J. Exp. Med.* 178:367–372.
10. Lawrence, M.B., E.L. Berg, E.C. Butcher, and T.A. Springer. 1995. Rolling of lymphocytes and neutrophils on peripheral node addressin and subsequent arrest on ICAM-1 in shear flow. *Eur. J. Immunol*. 25:1025–1031.
11. Bargatze, R.F., M.A. Jutila, and E.C. Butcher. 1995. Distinct roles of L-selectin and integrins $\alpha4\beta7$ and LFA-1 in lymphocyte homing to Peyer's patch–HEV in situ: the multistep model confirmed and refined. *Immunity*. 3:99–108.
12. Arbonès, M.L., D.C. Ord, K. Ley, H. Ratech, C. Maynard-Curry, G. Otten, D.J. Capon, and T.F. Tedder. 1994. Lymphocyte homing and leukocyte rolling and migration are impaired in L-selectin–deficient mice. *Immunity*. 1:247–260.
13. Wagner, N., J. Lohler, E.J. Kunkel, K. Ley, E. Leung, G. Krissansen, K. Rajewsky, and W. Müller. 1996. Critical role for β7 integrins in formation of the gut-associated lymphoid tissue. *Nature*. 382:366–370.
14. Gallatin, W.M., I.L. Weissman, and E.C. Butcher. 1983. A cell-surface molecule involved in organ-specific homing of lymphocytes. *Nature*. 304:30–34.
15. Streeter, P.R., B.T.N. Rouse, and E.C. Butcher. 1988. Immunohistologic and functional characterization of a vascular addressin involved in lymphocyte homing into peripheral lymph nodes. *J. Cell Biol*. 107:1853–1862.
16. Tedder, T.F., D.A. Steeber, and P. Pizcueta. 1995. L-selectin–deficient mice have impaired leukocyte recruitment into inflammatory sites. *J. Exp. Med*. 181:2259–2264.
17. Catalina, M.D., M.C. Carroll, H. Arizpe, A. Takashima, P. Estess, and M.H. Siegelman. 1996. The route of antigen entry determines the requirement for L-selectin during immune responses. *J. Exp. Med*. 184:2341–2351.
18. Xu, J., I.S. Grewal, G.P. Geba, and R.A. Flavell. 1996. Impaired primary T cell responses in L-selectin–deficient mice. *J. Exp. Med*. 183:589–598.
19. Hamann, A., D.J. Westrich, A. Duijevstijn, E.C. Butcher, H. Baisch, R. Harder, and H.G. Thiele. 1988. Evidence for an accessory role of LFA-1 in lymphocyte–high endothelium interaction during homing. *J. Immunol*. 140:693–699.
20. Schmits, R., T.M. Kundig, D.M. Baker, G. Shumaker, J.J. Simard, G. Duncan, A. Wakeham, A. Shahinian, A. van der Heiden, M.F. Bachmann, et al. 1996. LFA-1–deficient mice show normal CTL responses to virus but fail to reject immunogenic tumor. *J. Exp. Med*. 183:1415–1426.
21. Spangrude, G.J., B.A. Braaten, and R.A. Daynes. 1984. Mo-

lecular mechanisms of lymphocyte extravasation. I. Studies of two selective inhibitors of lymphocyte recirculation. *J. Immunol.* 132:354–362.
22. Chaffin, K.E., C.R. Beals, T.M. Wilkie, K.A. Forbush, M.I. Simon, and R.M. Perlmutter. 1990. Dissection of thymocyte signaling pathways by in vivo expression of pertussis toxin ADP-ribosyltransferase. *EMBO (Eur. Mol. Biol. Organ.) J.* 9: 3821–3829.
23. Pizza, M., A. Covacci, A. Bartoloni, M. Perugini, L. Nencioni, M.T. De Magistris, L. Villa, D. Nucci, R. Manetti, and M. Bugnoli. 1989. Mutants of pertussis toxin suitable for vaccine development. *Science*. 246:497–500.
24. Sanchez-Madrid, F., P. Simon, S. Thompson, and T.A. Springer. 1983. Mapping of antigenic and functional epitopes on the α and β subunits of two related glycoproteins involved in cell interactions, LFA-1 and Mac-1. *J. Exp. Med.* 158:586–602.
25. von Andrian, U.H. 1996. Intravital microscopy of the peripheral lymph node microcirculation in mice. *Microcirculation*. 3:287–300.
26. Pries, A.R. 1988. A versatile video image analysis system for microcirculatory research. *Int. J. Microcirc. Clin. Exp.* 7:327–345.
27. Stewart, M., and N. Hogg. 1996. Regulation of leukocyte integrin function: Affinity vs. avidity. *J. Cell. Biochem.* 61: 554–561.
28. von Andrian, U.H., P. Hansell, J.D. Chambers, E.M. Berger, I.T. Filho, E.C. Butcher, and K.E. Arfors. 1992. L-selectin function is required for β_2-integrin–mediated neutrophil adhesion at physiological shear rates in vivo. *Am. J. Physiol.* 263:H1034–H1044.
29. Kanwar, S., D.C. Bullard, M.J. Hickey, C. Wayne Smith, A.L. Beaudet, B.A. Wolitzky, and P. Kubes. 1997. The association between α_4-integrin, P-selectin, and E-selectin in an allergic model of inflammation. *J. Exp. Med.* 185:1077–1087.
30. De Bruyn, P.P., and Y. Cho. 1990. Structure and function of high endothelial postcapillary venules in lymphocyte circulation. *Nature*. 84:85–101.
31. Marchesi, V.T., and J.L. Gowans. 1963. The migration of lymphocytes through the endothelium of venules in lymph nodes: an electron microscope study. *Proc. R. Soc. Lond. B. Biol.* 159:283–290.
32. Kikuta, A., and S.D. Rosen. 1994. Localization of ligands for L-selectin in mouse peripheral lymph node high endothelial cells by colloidal gold conjugates. *Blood*. 84:3766–3775.
33. Sasaki, K., Y. Okouchi, H.-J. Rothkötter, and R. Pabst. 1996. Ultrastructural localization of the intercellular adhesion molecule (ICAM-1) on the cell surface of high endothelial venules in lymph nodes. *Anat. Rec.* 244:105–111.
34. Laudanna, C., G. Constantin, P. Baron, E. Scarpini, G. Scarlato, G. Cabrini, C. Dechecchi, F. Rossi, M.A. Cassatella, and G. Berton. 1994. Sulfatides trigger increase of cytosolic free calcium and enhanced expression of tumor necrosis factor-α and interleukin-8 mRNA in human neutrophils. *J. Biol. Chem.* 269:4021–4026.
35. Brenner, B., E. Gulbins, K. Schlottmann, U. Koppenhoefer, G.L. Busch, B. Walzog, M. Steinhausen, K.M. Coggeshall, O. Linderkamp, and F. Lang. 1997. L-selectin activates the Ras pathway via the tyrosine kinase p56lck. *Proc. Natl. Acad. Sci. USA*. 93:15376–15381.
36. Sikorski, M.A., D.E. Staunton, and J.W. Mier. 1996. L-selectin crosslinking induces integrin-dependent adhesion: evidence for a signaling pathway involving PTK but not PKC. *Cell Adhes. Commun.* 4:355–367.
37. Hwang, S.T., M.S. Singer, P.A. Giblin, T.A. Yednock, K.B. Bacon, S.I. Simon, and S.D. Rosen. 1996. GlyCAM-1, a physiologic ligand for L-selectin, activates β 2 integrins on naive peripheral lymphocytes. *J. Exp. Med.* 184:1343–1348.
38. Picker, L.J., and E.C. Butcher. 1992. Physiological and molecular mechanisms of lymphocyte homing. *Annu. Rev. Immunol.* 10:561–591.
39. Williams, M.B., and E.C. Butcher. 1997. Homing of naïve and memory T lymphocyte subsets to Peyer's patches, lymph nodes, and spleen. *J. Immunol.* 159:1746–1752.
40. Mackay, C. 1993. Homing of naive, memory and effector lymphocytes. *Curr. Opin. Immunol.* 5:423–427.
41. Diacovo, T.G., K.D. Puri, R.A. Warnock, T.A. Springer, and U.H. von Andrian. 1996. Platelet-mediated lymphocyte delivery to high endothelial venules. *Science*. 273:252–255.
42. Diacovo, T.G., M.D. Catalina, M.H. Siegelman, and U.H. von Andrian. 1998. Circulating activated platelets reconstitute lymphocyte homing and peripheral immunity in L-selectin–deficient mice. *J. Exp. Med.* 187:197–204.
43. Shier, P., G. Otulakowski, K. Ngo, J. Panakos, E. Chourmouzis, L. Christjansen, C.Y. Lau, and W.P. Fung-Leung. 1996. Impaired immune responses toward alloantigens and tumor cells but normal thymic selection in mice deficient in the β2 integrin leukocyte function-associated antigen–1. *J. Immunol.* 157:5375–5386.
44. Dustin, M.L., and T.A. Springer. 1989. T cell receptor cross-linking transiently stimulates adhesiveness through LFA-1. *Nature*. 341:619–624.
45. van Kooyk, Y., P. van de Wiel-van Kemenade, P. Weder, T.W. Kuijpers, and C.G. Figdor. 1989. Enhancement of LFA-1–mediated cell adhesion by triggering through CD2 or CD3 on T lymphocytes. *Nature*. 342:811–813.
46. Laudanna, C., J.J. Campbell, and E.C. Butcher. 1996. Role of Rho in chemoattractant-activated leukocyte adhesion through integrins. *Science*. 271:981–983.
47. Campbell, J.J., J. Hedrick, A. Zlotnik, M.A. Siani, D.A. Thompson, and E.C. Butcher. 1998. Novel chemokines trigger rapid arrest of rolling lymphocytes under physiologic shear. *Science*. In press.
48. Nickoloff, B.J., and R.S. Mitra. 1988. Phorbol ester treatment enhances binding of the mononuclear leukocytes to autologous and allogenic gamma-interferon–treated keratinocytes, which are blocked by anti–LFA-1 monoclonal antibody. *J. Investig. Dermatol.* 90:684–689.
49. Andrew, D.P., C. Berlin, S. Honda, T. Yoshino, A. Hamann, B. Holzmann, P.J. Kilshaw, and E.C. Butcher. 1994. Distinct but overlapping epitopes are involved in α4β7-mediated adhesion to vascular cell adhesion molecule-1, mucosal addressin-1, fibronectin, and lymphocyte aggregation. *J. Immunol.* 153:3847–3861.
50. Jung, T.M., W.M. Gallatin, I.L. Weissman, and M.O. Dailey. 1988. Down-regulation of homing receptors after T cell activation. *J. Immunol.* 141:4110–4117.
51. Lewinsohn, D.M., R.F. Bargatze, and E.C. Butcher. 1987. Leukocyte-endothelial cell recognition: evidence of a common molecular mechanism shared by neutrophils, lymphocytes, and other leukocytes. *J. Immunol.* 138:4313–4321.
52. May, M.J., G. Entwistle, M.J. Humphries, and A. Ager. 1993. VCAM-1 is a CS1 peptide-inhibitable adhesion molecule expressed by lymph node high endothelium. *J. Cell. Sci.* 106:109–119.
53. Szabo, M.C., E.C. Butcher, and L.M. McEvoy. 1997. Specialization of mucosal follicular dendritic cells revealed by

mucosal addressin-cell adhesion molecule-1 display. *J. Immunol.* 158:5584–5588.
54. Hahne, M., M. Lenter, U. Jäger, S. Isenmann, and D. Vestweber. 1993. VCAM-1 is not involved in LPAM-1 (α4βp/α4β7) mediated binding of lymphoma cells to high endothelial venules of mucosa-associated lymph nodes. *Eur. J. Cell. Biol.* 61:290–298.
55. Nakache, M., E.L. Berg, P.R. Streeter, and E.C. Butcher. 1989. The mucosal vascular addressin is a tissue-specific endothelial cell adhesion molecule for circulating lymphocytes. *Nature*. 337:179–181.
56. Hamann, A., D.P. Andrew, D. Jablonski-Westrich, B. Holzmann, and E.C. Butcher. 1994. Role of α4-integrins in lymphocyte homing to mucosal tissues in vivo. *J. Immunol.* 152: 3282–3293.
57. Hamann, A., D. Jablonski-Westrich, P. Jonas, and H.-G. Thiele. 1991. Homing receptors reexamined: mouse LECAM-1 (MEL-14 antigen) is involved in lymphocyte migration into gut-associated lymphoid tissue. *Eur. J. Immunol.* 21:2925–2929.
58. Miura, S., Y. Tsuzuki, I. Kurose, M. Suematsu, T. Shigematsu, H. Kimura, H. Higuchi, H. Serizawa, H. Yagita, K. Okumura, et al. 1996. Endotoxin stimulates lymphocyte-endothelial interactions in rat intestinal Peyer's patches and villus mucosa. *Am. J. Physiol.* 271:G282–G292.
59. Jalkanen, S., R.F. Bargatze, J. de los Toyos, and E.C. Butcher. 1987. Lymphocyte recognition of high endothelium: antibodies to distinct epitopes of an 85–95 kD glycoprotein antigen differentially inhibit lymphocyte binding to lymph node, mucosal and synovial endothelial cells. *J. Cell Biol.* 105:983–993.
60. McEvoy, L.M., H. Sun, J.G. Frelinger, and E.C. Butcher. 1997. Anti-CD43 Inhibition of T Cell Homing. *J. Exp. Med.* 185:1493–1498.
61. Salmi, M., and S. Jalkanen. 1996. Human vascular adhesion protein 1 (VAP-1) is a unique sialoglycoprotein that mediates carbohydrate-dependent binding of lymphocytes to endothelial cells. *J. Exp. Med.* 183:569–579.